Determining the number of integrals of motion by an adapted correlation dimension method

Johannes Floß and Paul Brumer
Chemical Physics Theory Group, Department of Chemistry, and Center for Quantum Information and Quantum Control, University of Toronto, Toronto, Ontario M5S 3H6, Canada

(Received 15 November 2018; published 28 March 2019)

An adapted correlation dimension algorithm is used to numerically determine the number of integrals of motion in a variety of conservative classical systems. The method is demonstrated on three sample systems that display various degrees of integrable and chaotic behavior: the Hénon-Heiles Hamiltonian, an asymmetric top molecule in an electric field, and the planetary system HD128311. Two additional applications of the method emerge: using the adapted correlation dimension algorithm (a) to study partial barriers and turnstiles in phase space and (b) to predict the long-time stability of planetary systems using short-time data.

DOI: 10.1103/PhysRevE.99.032222

I. INTRODUCTION

Among the most important properties of a physical system are its integrals of motion; even knowledge of the *number of integrals* of motion can greatly help to understand a system's dynamics. For example, it can reveal whether different degrees of freedom are coupled or not and whether the dynamics are regular or chaotic. Significantly, knowing the number of integrals of motion implies whether all integrals of motion for a particular system have been found or not. A prominent example of the latter is the search for a third integral of motion in celestial dynamics [1].

Finding the number of integrals of motion is, in general, a nontrivial task. For example, in using analytical methods it equates to finding the integrals of motion themselves, practically impossible for all but for the simplest systems. It is therefore of great interest to have a numerical tool to find the number of integrals of motion, and, as a consequence, a variety of methods have been proposed [2–6]. They all rely on the fact that a trajectory in a classical conservative system traces out a surface S of dimension ν. This dimension is linked to the number C of the integrals of motion via

$$\nu = 2d - C, \tag{1}$$

where d is number of degrees of freedom and $2d$ is the dimension of the embedding phase space. A numerical method that can determine ν can thus also be used to determine C.

One of the first attempts to numerically obtain the number of integrals of motion was due to Stine and Noid [2], who used a box-counting algorithm to determine ν. They succesfully demonstrated this technique for selected trajectories in the Hénon-Heiles system [7]. However, the large numerical demands of the box-counting algorithm limits this approach to very low dimensional systems. Subsequently, Martens and Ezra [4] applied the pointwise dimension method [8] to calculate ν, which is numerically much more efficient than the box-counting algorithm. However, it uses only a few selected points on a trajectory and could thus overlook different behavior at different parts of phase space.

Around the same time, Grassberger and Procaccia developed the correlation dimension method to characterize strange attractors [9]. This method gives a higher weight to regions of phase space that are visited more often by a trajectory, thus possibly yielding a different value for the dimension ν than the box-counting or pointwise dimension methods. Carnevali and Santangelo proposed [3] using the correlation dimension method to determine the number of integrals of motion, testing their proposal on a small number of selected trajectories in the Hénon-Heiles system. Their study was later extended to other low-dimensional systems [5] and large ensembles of trajectories [6] modeling planetary motion.

In this article, we extend and apply the correlation dimension method to determine the dimension ν, and thereby the number of integrals of motion, of three dramatically different systems. In contrast with previous studies, an additional step is introduced to ensure that all parts of the surface S on which the trajectory evolves are equally weighted, ensuring better access to the number of integrals. Thus, our approach combines the numerical efficiency of the correlation dimension method with the accuracy of the box-counting method. Additionally, we show applications of this method not reported earlier, including determining diffusion times through phase space barriers and predicting the stability of planetary systems with very short time measurements.

The method is first applied to the Hénon-Heiles system in both regular and chaotic regimes (Sec. III), allowing us to compare the adapted approach to previous studies; good agreement is found. Furthermore, and significantly, the results show the existence of partial barriers in phase space. The second example, an asymmetric top molecular rotor in an external electric field (Sec. IV), demonstrates the success of the method for integrable and chaotic rotational systems. The proposed method is also seen capable of revealing quasi-isolating integrals of motion. Finally, a planetary system is investigated (Sec. V), showing that the method can be used to predict the stability of such a system over a long time by using only very short time data. Remarkably, only 25 orbital cycles were needed for this prediction, opening the possibility of using experimentally observable data. Section II

 ©2019 American Physical Society

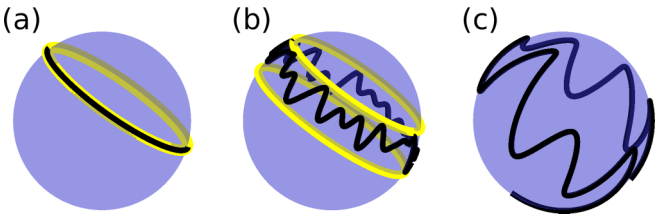

FIG. 1. A sketch to illustrate isolating and quasi-isolating integrals of motion, using trajectories in a three-dimensional phase space at fixed energy E. The trajectories are bound to move on the two-dimensional energy surface, here a (blue) sphere. (a) An isolating integral of motion (bright yellow circle) restricts the trajectory (black line) onto a one-dimensional subspace of the energy surface. (b) A quasi-isolating integral of motion (bright yellow circles) restricts the trajectory (black line) to a subspace of the energy surface; however, this subspace is also two-dimensional. (c) If no additional isolating integral of motion exists, the trajectory can cover the whole energy surface.

provides a short review of the correlation dimension method, including the modifications for the present study, prior to presenting these results for the three-sample system. Note that the algorithm can be applied to any desired set of trajectories. This can be an ensemble of trajectories typical for a system (as in Secs. III and IV), trajectories spanning a parameter space (as in Sec. V), or also a single special trajectory like a separatrix.

Note that in this article, by integrals of motion we only mean isolating and quasi-isolating ones as defined in Refs. [10,11], since nonisolating integrals are of no physical interest. Figure 1 provides some insight into the difference between isolating and quasi-isolating integrals of motion. An isolating integral of motion reduces the dimensionality of occupiable phase space. Consider an N-dimensional phase space at fixed energy E; trajectories would cover an $N-1$ dimensional surface. An additional isolating integral of motion would reduce the space covered by a trajectory to dimension $N-2$. This situation is depicted in Fig. 1(a): The trajectory on a *two*-dimensional energy surface is forced by the additional isolating integral of motion to lie on a *one*-dimensional subspace of the energy surface. By contrast, a quasi-isolating integral of motion would allow trajectories to cover a phase space dimension of $N-1$, but they would not cover all of the $(N-1)$-dimensional space, i.e., they would not be ergodic on the fixed energy manifold. This case is depicted in Fig. 1(b): The quasi-isolating integral limits the trajectory to a subspace of the *two*-dimensional energy surface, with this subspace also being *two*-dimensional. Only in the absence of any additional integral of motion, the trajectory can cover the whole energy surface, as depicted in Fig. 1(c).

II. THE CORRELATION DIMENSION METHOD

The correlation dimension algorithm was developed to characterize strange attractors [9], as an alternative to the box-counting method [12]. While the latter has the advantage of yielding the exact geometric dimension of any surface, it is very inefficient numerically and thus limited to at most three-dimensional structures. Below we summarize the correlation dimension algorithm and our modification designed to obtain the number of integrals of motion rather than the correlation dimension. A good introduction to the numerical implementation of the original approach is provided by Sprott [13].

Consider a system with d degrees of freedom and thus a $2d$-dimensional phase space with coordinates q_i and momenta p_i. A classical trajectory $\mathbf{X}(t) = (q_1(t), q_2(t), \ldots, q_d(t), p_1(t), p_2(t), \ldots, p_d(t))$ traces out a ν-dimensional surface S in phase space. In order to numerically determine ν, one has to obtain a set $\{\mathbf{X}_n\}$ of points lying on S. A simple way is to propagate the trajectory and select points at regular time intervals τ: $\mathbf{X}_n = \mathbf{X}(n\tau)$. One then calculates the correlation sum $C(l)$, which counts the number of all pairs $(\mathbf{X}_m, \mathbf{X}_n)$ with a distance smaller than l:

$$C(l) = A \sum_{\substack{m,n=1 \\ |m-n|>s}}^{N} \Theta(l - |\mathbf{X}_m - \mathbf{X}_n|). \tag{2}$$

Here N is the number of phase space points in the set $\{\mathbf{X}_n\}$, Θ is the Heaviside step function, and A is a normalization factor. The parameter s provides a minimal temporal separation between points of the trajectory: To avoid short-time temporal correlations influencing the algorithm [14], only phase space point pairs $(\mathbf{X}_m, \mathbf{X}_n)$ with a temporal separation $\Delta t = |m-n|\tau$ larger than $s\tau$ are included in the correlation sum. In this work, the values chosen for τ are sufficiently large to use $s = 1$ for the Hénon-Heiles system as well as the asymmetric top rotor; for the planetary system HD128311 $s = 1000$ was used.

The original algorithm [9] puts a higher emphasis on phase space regions that are visited more frequently by the trajectory, and thus the algorithm may yield a lower dimension for the surface S than its geometric dimension. However, in order to obtain the number of integrals of motion, the latter is required. Thus, in this work the algorithm is modified by including an additional scaling following the idea of Monte Carlo sampling on an energy surface [15]: individual points were removed from the set $\{\mathbf{X}_n\}$ to ensure a uniform coverage of the surface S by the set. Specifically, a point $\mathbf{X}_n$ on the trajectory was included in the set if the phase space velocity $d\mathbf{X}/dt$ at this point was larger than a random number r uniformly distributed between 0 and the largest measured phase space velocity.

The relation between $C(l)$ and the dimension ν is given, for sufficiently small $l > 0$, by [9]

$$C(l) \propto l^{\nu}. \tag{3}$$

Mind that the smaller l, the larger N has to be to overcome noise, increasing computational costs. Using Eq. (3), the dimension ν can be obtained numerically by a linear fit of $\log C$ over $\log l$. Specifically, a least squares linear fit for $\log(C)$ versus $\log(l)$ is done on an interval $\log(l_0) < \log(l) < \log(l_0) + 0.5$, yielding $\nu(l_0)$ and the square error $\Delta(l_0)$ within this interval. The parameter l_0 is then scanned within an interval $[l_1, l_2]$ of interest, and the value l_0 for which $\Delta(l_0)$ is minimal is chosen to provide the final value for ν.

Figure 2 shows three typical cases that can be encountered when determining ν from $C(l)$. Figure 2(a) depicts the "ideal" case. Here the phase space structure traced out by the trajectory has the same dimension over all length scales, and this dimension is a function of the number of integrals of motion [namely, Eq. (1)].

When quasi-isolating integrals of motion are present, ν can take on different values at different l. Such an integral does not restrict the trajectory to a lower-dimensional surface as in the case of an isolating integral, but it does limit the region the trajectory can explore (see Sec. I). Most importantly, a quasi-isolating integral prevents the trajectory from passing close to every point of the surface defined by the isolating integrals of motion, thus making the system nonergodic [10]. At short length scales the quasi-isolating integral does not matter, and the dimension ν depends on the number of isolating integrals only. At long scales ν can depend upon both isolating and quasi-isolating integrals [16]. Consequently, in the presence of a quasi-isolating integral of motion the dimension ν may change with l (though it does not have to); in particular ν may become smaller at larger l. This situation is depicted in Fig. 2(b). The adapted correlation dimension method thus can discern multivariable size phase space structures. Note that also for the original correlation dimension method the observation of different dimensions at different lengths scales was reported [17].

If a trajectory is sampled at intervals shorter than the typical period of the system, points lying close in time will also lie close in space; thus, at small l the correlation dimension algorithm is likely to pick up correlations between points close in time [14]. However, on a short timescale a trajectory does not densely cover the surface it evolves on, it reveals only the one-dimensional structure of the trajectory itself. This can lead to $\nu = 1$ at small l, and the real dimension ν of the underlying surface is revealed only at large l; this situation is depicted in Fig. 2(c). In order to avoid these temporal correlations, the parameter s was introduced (see above). Note that it is also possible to have an actual dimension of $\nu = 1$ (with a correspondingly large number of isolating integrals of motion) at small l, e.g., when the trajectory is periodic in time.

A note regarding the scaling of the coordinates and momenta: It is always necessary to introduce such a scaling to obtain a phase space metric. In the original algorithm [9], the dimension was determined in the limit $l \to 0$, and thus the choice of the metric had no influence. This is no longer true when using this algorithm to determine the number of integrals of motion, as the choice of the metric influences at which phase space distance a quasi-isolating integral starts to have an effect. It is therefore advisable to always check which influence the chosen metric has on the resulting number of integrals of motion.

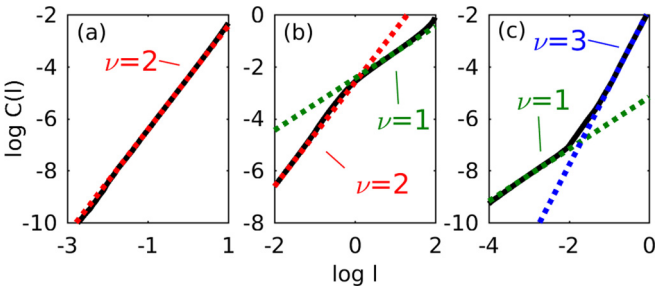

FIG. 2. Three examples for determining the dimension ν from the correlation sum $C(l)$ (see text). The solid line depicts the correlation sum, the dotted lines are linear fits with slope ν.

III. HÉNON-HEILES SYSTEM

The Hénon-Heiles system was introduced in the search for a third integral of celestial motion [7] and is one of the first systems in which the transition from regular to chaotic motion was observed, including in molecular systems [18]. Since its inception, it has become a standard system in the study of chaotic dynamics and has also been used in previous studies on numerically obtaining the integrals of motion [2–6].

The Hénon-Heiles system has two degrees of freedom and is defined by the potential

$$V(x, y) = (x^2 + y^2)/2 + \lambda(x^2 y - y^3/3), \tag{4}$$

shown in Fig. 3. Here λ is a parameter which, in the following, is set to $1/\sqrt{80}$. The Hénon-Heiles potential has a local potential well centered at $(x = 0, y = 0)$. Motion bounded in this well, as considered here, occurs only below the escape energy $E_e = 1/(6\lambda^2) \approx 13.33$; the area of bounded motion is marked by dashed lines in Fig. 3.

At energies below a critical energy E_c (here $\approx 0.6E_e$) the dynamics of the Hénon-Heiles system is almost completely regular [7]; above E_c both regular and chaotic dynamics are present (see, e.g., Ref. [18]). The extent of the chaotic regions of phase space increases with increasing energy.

For all trajectories, the energy E is an integral of motion. Additionally, the trajectories with regular dynamics have a second integral of motion, the so-called "third integral" [7]. Since the system has two degrees of freedom and thus a four-dimensional phase space, it is expected that the regular trajectories evolve on two-dimensional and the chaotic ones on three-dimensional surfaces. The relative amount of two- and three-dimensional trajectories is expected to follow the pattern of regular and chaotic dynamics: (almost) only two-dimensional trajectories for $E < E_c$, and an increasing

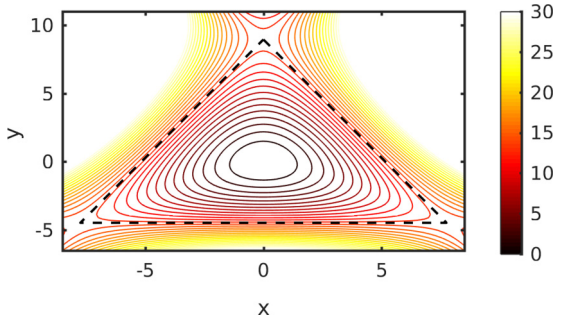

FIG. 3. Equipotential lines for the Hénon-Heiles potential, using the parameters mentioned in the text. The dashed lines enclose the area of bound trajectories. The color scale yields the value of the potential.

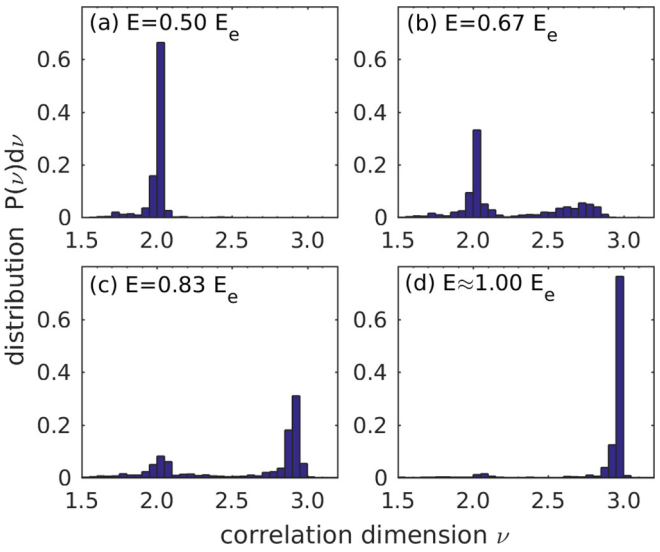

FIG. 4. Distribution $P(\nu)$ of the correlation dimension ν for the Hénon-Heiles system, at different energies E. The dimensions are calculated for a random sample of 1000 trajectories, with set sizes of $N = 64\,000$, and $e^{-3} \leqslant l_0 \leqslant e^{-1}$.

fraction of three-dimensional trajectories with increasing energy.

To determine the dimension of the dynamics, 1000 random trajectories at a given energy E were calculated and their dimension ν determined with the algorithm described above. The numerical parameters were chosen as $\tau = 1$, $s = 1$, and $N = 64\,000$, and there was no scaling of coordinates and momenta. All trajectories were found to have a single linear slope [as in Fig. 2(a)], although the value of ν varied between different trajectories. In Fig. 4 histograms of the trajectories' dimensions for four different energies are shown. The results support the above perspective: All histograms show peaks at $\nu = 2$ and/or $\nu = 3$, corresponding to regular and chaotic dynamics, respectively. (In additional calculations, using exponential divergence as a chaos indicator [19], it was verified that the trajectories with $\nu \approx 2$ are indeed regular, and trajectories with $\nu \approx 3$ are indeed chaotic.) The dependence on the energy mirrors the regular to chaotic transition: At energies below E_c, only two-dimensional trajectories were found; at energies close to E_e, almost all trajectories show three-dimensional dynamics; and at intermediate energies, the ratio of two- to three-dimensional trajectories decreases with increasing energy.

An interesting aspect can be found at energies just above the critical energy, as depicted in Fig. 4(b): The upper peak, which would be associated with chaotic trajectories, is not found at $\nu = 3$, but at a fractal value of $\nu \approx 2.7$. The peak is also rather broad. Such a fractal dimension for the chaotic trajectories in the Hénon-Heiles system was also observed in previous studies that tried to determine the number of integrals of motion by the correlation dimension method [3,5,6]. This fractal dimension has been interpreted in the past as the result of quasi-ergodicity [5]—defined as orbits that are almost ergodic but "have some (unknown) restriction in addition to that of their ergodic cousins"—or as the result of switching between two-dimensional regular and three-dimensional chaotic dynamics [6]. Below, we provide a different interpretation.

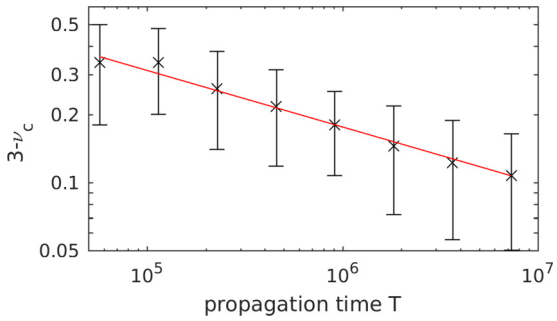

FIG. 5. Convergence towards the integer value of 3 of the position ν_c of the upper peak in the histograms of the dimensions of the Hénon-Heiles system at $E = 0.67E_e$, as a function of the total sampling time T. The solid red line depicts the curve $5.6/\sqrt[4]{T}$.

Since the correlation dimension method gives different weights to different parts of the surface S upon which the trajectory evolves, it can yield fractal dimensions even in a system with an integer number of isolating integrals of motion [9]. However, the method employed here corrects for the weighting of the correlation dimension method, and thus no fractal values for ν should be found. Nonetheless, as seen in Fig. 4(b), they are; this apparent contradiction is discussed immediately below.

An alternate interpretation to the quasi-ergodicity theory that could explain why a fractal dimension was also observed here is as follows. Assume that the surface S that a chaotic trajectory can access is split into small regions (S_A, S_B, S_C,...) that are connected via turnstiles or partial barriers [20–22]. The trajectory starts at time t_0 in region S_A and fills it ergodically. At time t_1, which is larger than the timescale of the evolution within S_A, the trajectory jumps to region S_B, starting to trace out this part of the surface S. Shortly after t_1 the correlation sum includes more points from subsurface S_A than from S_B, and the different weights of different parts of S leads to a fractal value of ν. At a later time t_2 the trajectory has covered S_B to the same degree as S_A, and ν as determined by the correlation dimension method becomes integer, unless the trajectory jumped again, to subsurface S_C, leading again to an uneven coverage of S. Only after a very long observation time, sufficiently long that the trajectory visited every region, all parts of S are covered evenly, and the correlation dimension method is capable of determining the "true" dimension of S. This behavior is likely related to "stickiness" [23].

To test this interpretation, the calculation of the dimension for $E = 0.67E_e$ was done repeatedly, each time increasing the distance τ between the sampled phase space points and thus increasing the total time $T \approx N\tau$ over which the sample was acquired. In Fig. 5 the difference of the position ν_c of the upper peak of the histogram and $\nu = 3$ is shown as a function of T. It can be found to decrease as approximately $1/\sqrt[4]{T}$, and thus the dimension ν_c indeed approaches the integer value of 3 with time, supporting the above interpretation of the fractal values. Note that there is no general rule for the timescale of passing through partial phase space barriers, anything from exponential to power laws is possible [22].

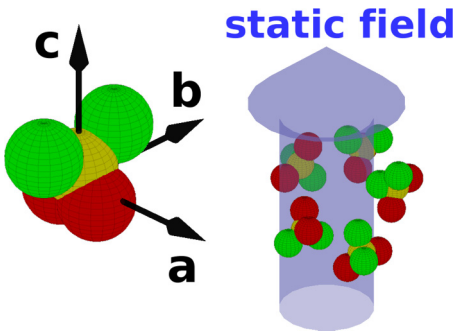

FIG. 6. A sketch of the second example system: An asymmetric top molecular rotor in a static electric field. In this work a hypothetical molecule is considered with a permanent dipole moment pointing along the c axis of the molecular frame.

IV. ASYMMETRIC TOP MOLECULE IN AN ELECTRIC FIELD

The second system investigated in this study is a rigid asymmetric top molecule in a static electric field, as illustrated in Fig. 6. The Hamiltonian of this system describing the free rotation and the interaction between the electric field and the molecule's permanent dipole moment is given as

$$H = \frac{J_a^2}{2I_a} + \frac{J_b^2}{2I_b} + \frac{J_c^2}{2I_c} + \frac{\Phi}{2}(1 - \cos\theta). \tag{5}$$

Here J_i is the projection of the angular momentum on the ith axis of the molecular frame, I_i is the moment of inertia along this axis, Φ is the potential well depth of the field-dipole interaction, and θ is the angle between the molecular dipole and the electric field. Note that in the following Φ is given in units of the total energy E_{tot}. A hypothetical molecule is considered, with $I_a = 1/8$, $I_b = 2/8$, $I_c = 5/8$ (in units of the total moment of inertia) and a dipole moment pointing along the c axis. For the numerical treatment and calculation of phase space distances Euler parameters and their conjugate momenta are used. The former are given as [24]

$$q_0 = \cos\left(\frac{\phi+\chi}{2}\right)\cos\left(\frac{\theta}{2}\right), \tag{6a}$$

$$q_1 = \sin\left(\frac{\phi-\chi}{2}\right)\sin\left(\frac{\theta}{2}\right), \tag{6b}$$

$$q_2 = \cos\left(\frac{\phi-\chi}{2}\right)\sin\left(\frac{\theta}{2}\right), \tag{6c}$$

$$q_3 = \sin\left(\frac{\phi+\chi}{2}\right)\cos\left(\frac{\theta}{2}\right), \tag{6d}$$

where θ, ϕ, and χ are the Euler angles using the y convention [24]. The conjugate momenta are given as [25]

$$p_0 = -2q_1J_a - 2q_2J_b - 2q_3J_c, \tag{7a}$$

$$p_1 = 2q_0J_a + 2q_2J_c - 2q_3J_b, \tag{7b}$$

$$p_2 = 2q_0J_b + 2q_3J_a - 2q_1J_c, \tag{7c}$$

$$p_3 = 2q_0J_c + 2q_1J_b - 2q_2J_a. \tag{7d}$$

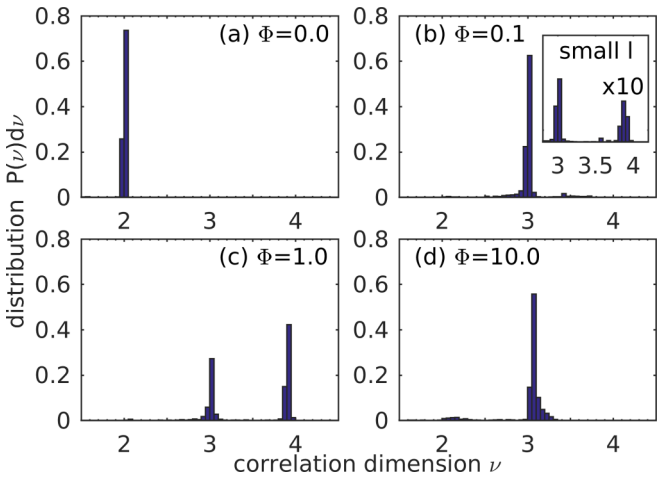

FIG. 7. Distribution $P(\nu)$ of the correlation dimension ν for an asymmetric top molecule in an electric field at different interaction strengths Φ. The histograms are calculated for a random sample of 1000 trajectories, with set sizes of $N = 256\,000$, and $e^{-5} \leqslant l_0 \leqslant e^{-2}$. The inset in panel (b) shows the result for small distances only, with $l_0 \leqslant e^{-5}$ (no scanning) and $N = 1\,024\,000$; the peak at $\nu \approx 4$ is enlarged by a factor of 10.

The trajectory $(\mathbf{q}(t), \mathbf{p}(t))$ is calculated by the method described in Ref. [26]. The momenta are furthermore scaled by $\sqrt{8E_{\text{tot}}I_{\text{tot}}}$, which ensures that the Euler parameters and their conjugate momenta are all approximately within the range $[-1, 1]$. The other parameters of the algorithm are (where not mentioned) $\tau = 0.1$, $s = 1$, and $N = 256\,000$; here τ is in units of $\sqrt{I_{\text{tot}}/E_{\text{tot}}}$.

The asymmetric top rigid molecule is a three degree of freedom system and thus has a six-dimensional phase space. Without the electric field, there are four isolating integrals of motion—the total energy E_{tot} as well as the three components of the angular momentum $\mathbf{J}$—and thus the trajectories are expected to lie on two-dimensional surfaces. In Fig. 7(a) a histogram of the dimension ν for 1000 random initial states of an asymmetric top rotor with no external field are shown. As expected, all trajectories evolve on two-dimensional surfaces.

Turning on the external field changes this situation abruptly. In Fig. 7(b) the histogram is shown for a weak field of $\Phi = 0.1$: There is still a single narrow peak, but it is shifted to the next integer value, i.e., $\nu = 3$. An abrupt change may be expected, but actually to $\nu = 4$: that is, when the field is turned on, the Hamiltonian (5) is known to have (at least) two isolating integrals of motion, the total energy and the component of the angular momentum along the electric field. Apparently, similar to the Hénon-Heiles system, there is an additional integral of motion. Also analogous to the Hénon-Heiles system, this additional integral is found in a regime of regular dynamics: As shown in previous studies [26,27], at $\Phi = 0.1$ most of the phase space is regular. Yet these studies have also shown that a small fraction of the phase space is chaotic even for a weak electric field, and thus one would expect a second peak at $\nu = 4$ in the histogram. Repeating the numerical procedure of the correlation dimension method, but this time restricting the length parameter l to very small values (and increasing N to 1 024 000 in order to reduce the noise at

small l), reveals a second peak at $\nu = 4$ [see inset of Fig. 7(b)]. A likely interpretation of this result is the existence of a quasi-isolating integral of motion (see Sec. II): There are chaotic trajectories evolving on four-dimensional surfaces; however, these chaotic regions are tightly enclosed by regular regions and thus follow the regular three-dimensional behavior on large length scales. Note that the analysis using the adopted correlation dimension method also reveals that the loss of the two integrals of motion by turning on the electric field is sudden and not smooth, as only one and not two quasi-isolating integrals are found at weak fields.

At a larger field strength of $\Phi = 1.0$ the dynamics are strongly mixed, around half of the phase space is chaotic, the other half regular [26]. The histogram for the dimensions is shown in Fig. 7(c), and it reflects the mixed phase space: There are two distinct peaks at $\nu = 3$ and $\nu = 4$, both of approximately the same size. In additional calculations it was found that the trajectories evolving on the three-dimensional surfaces are all regular, and the ones evolving on four-dimensional surfaces are all chaotic. Note that the peaks are clearly located at integer values of ν, there is no indication that the chaotic trajectories may have a fractal number of integrals of motion in this strongly mixed phase space.

Finally, at a very strong field of $\Phi = 10.0$, when the rotor is trapped deep within the potential well and regular dynamics prevail, the histogram returns to a single peak at $\nu = 3$ [see Fig. 7(d)], showing the return of a third integral of motion.

In summary, the correlation dimension method has revealed that the asymmetric top molecular rotor in an electric field is a mixed system with two clearly distinguishable regions in phase space: Regular regions with three integrals of motion, and chaotic regions with only two integrals of motion, the minimum number dictated by the symmetries of the Hamiltonian. At weak electric fields, the chaotic trajectories were found to have an additional quasi-isolating integral of motion, thus displaying a behavior similar to the regular trajectories. Notably, there are no trajectories evolving on a surface of fractal dimension, not even in a strongly mixed phase space, so there is no indication of phase space barriers as in the Hénon-Heiles system. This mixed phase space has also been found in a previous study using other indicators like Lyapunov exponents [26], however, without revealing the number of the integrals of motion.

V. STABILITY OF PLANETARY SYSTEMS

An important question for planetary systems is whether they are stable, i.e., whether the planetary orbits remain largely unaltered over astronomical timescales. Here we investigate whether the correlation dimension method can be used as a new tool to predict the stability of a planetary system, in particular if the system can be observed only over a short time, as is typical experimentally.

Consider a planetary system of N planets revolving around a star with a $6(N+1)$-dimensional phase space. This system is propagated over a short time (a few orbital cycles) to obtain the set $\{\mathbf{X}_n\}$, and the set's dimension in phase space is determined by the adapted correlation dimension method. The dimension obtained is unlikely to reveal the number of integrals of motion: Planetary systems are relatively large compared to the examples considered above (e.g., a two-planet system has already an 18-dimensional phase space), so very large sets of phase space points and long propagation times would be needed for an accurate determination; yet we consider a propagation over a short time only. However, quasi-isolating integrals may already be observable under these conditions. Furthermore, although one may not obtain the number of integrals of motion in a strict sense, i.e., the quantities that never change in the system, one does obtain the number of quantities that are conserved over the short observation time.

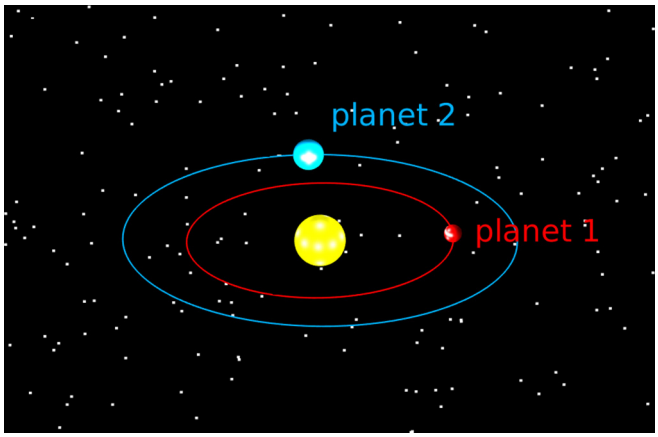

FIG. 8. Sketch of the third example: A system of two planets that orbit their central star in a co-planar setting. In particular, the parameters of the system HD128311 are used.

We suggest that the results from the short-time dynamics can foretell the systems' behavior on a long timescale, in particular that a large number of constants of motion during the short observation time correlates to stability of the system over a long time, and vice versa.

To test this claim, the planetary system of HD128311 is used as an example. It consists of two planets orbiting a single star in a coplanar setting [28,29], as illustrated in Fig. 8. After accounting for the coplanarity, the maximal phase space dimension of this systems is 12; there are six obvious integrals of motion (center of mass, energy, angular momentum), so that the highest dimension we may encounter is six. As initial conditions we used parameters provided in Ref. [30] but varied the eccentricity e_2 and the orbital period P_2 of the heavier planet, with the aim of determining the values of e_2 and P_2 for which the system would be stable. Using these initial parameters, the system was propagated over ~50 years (approximately 25 orbital cycles), using the REBOUND program package [31] with the IAS15 integrator [32]. Each of the coordinates and momenta were scaled to set its extension to 1: $\tilde{q}_i = q_i/[\max(q_i) - \min(q_i)]$ and $\tilde{p}_i = p_i/[\max(p_i) - \min(p_i)]$ (where the tilde denotes the scaled quantity). The obtained sets included $N = 64\,000$ points, obtained with a sampling period of $\tau = 0.05\,\text{years}/2\pi$. As stated above, since the trajectories were calculated over only a few orbital cycles, the correlation dimension method is unlikely to reveal the actual number of integrals of motion, but rather the (probably larger) number of quantities that are conserved over this short time. Furthermore, the short calculation time

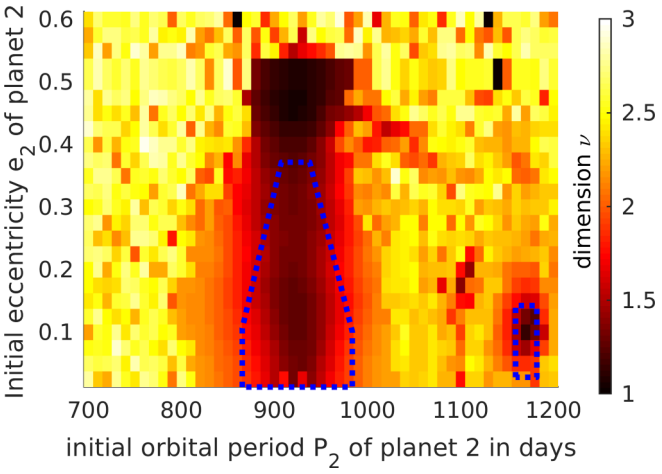

FIG. 9. Dimension ν as a function of the initial period P_2 and the initial eccentricity e_2 of the heavier planet of a two-planet system. The dotted lines approximately enclose the stable areas of the parameter space found in Ref. [30].

makes it harder to avoid temporal correlations [14], adding an additional source of error; to minimize temporal correlations, the parameter s was set rather high, to $s = 1000$. The obtained values should therefore not be interpreted as the number of integrals of motion of the system, but rather only as an indicator of the system's stability.

In Fig. 9 the calculated dimension is shown as a function of the heavier planet's initial orbital period P_2 and initial eccentricity e_2. The results show a sea of dimension $\nu \approx 2.5-3$, in which a large and a small island of lower dimensional dynamics are embedded. Following the above claim, the lower-dimensional areas are expected to be more stable than the higher-dimensional ones. In an earlier study [30] the stability of HD128311 was investigated by propagating the system over 100 000 years. A comparison of the present work's results with the stable areas of the parameter space reported in Ref. [30] (the borders of these areas are indicated by the dotted blue lines in Fig. 9) shows that the lower dimension indeed correlates with a larger stability.

For further illustration, in Fig. 10 the orbits of the two planets traced out over the simulation time are shown, for three different parameters: (a) $e_2 = 0.1, P_2 = 800$, in the unstable region; (b) $e_2 = 0.1, P_2 = 850$, between the stable and unstable region; and (c) $e_2 = 0.1, P_2 = 900$, in the stable region. In all three cases the planets are clearly interacting, since both planets do not trace out an invariable ellipse as would be seen in a noninteracting scenario. And although one can see a difference between the three cases—planet 2's orbit is less stable for the lower values of P_2—this difference is not qualitative, and it would be hard to predict which case is stable and which is not. The correlation dimension method, on the other hand, is able to translate these small differences into a qualitative criterion: A dimension of $\nu > 2$ is likely unstable, a dimension of $\nu < 2$ is likely stable.

Note that for the stability prediction presented here it was sufficient to obtain data for less than 25 orbital cycles. Additionally, the correlation dimension algorithm may also work when the time dependence of only a single coordinate is known [9]. In combination, this may allow for the correlation dimension method to predict stabilities of planetary systems using experimentally observable (i.e., short time) data.

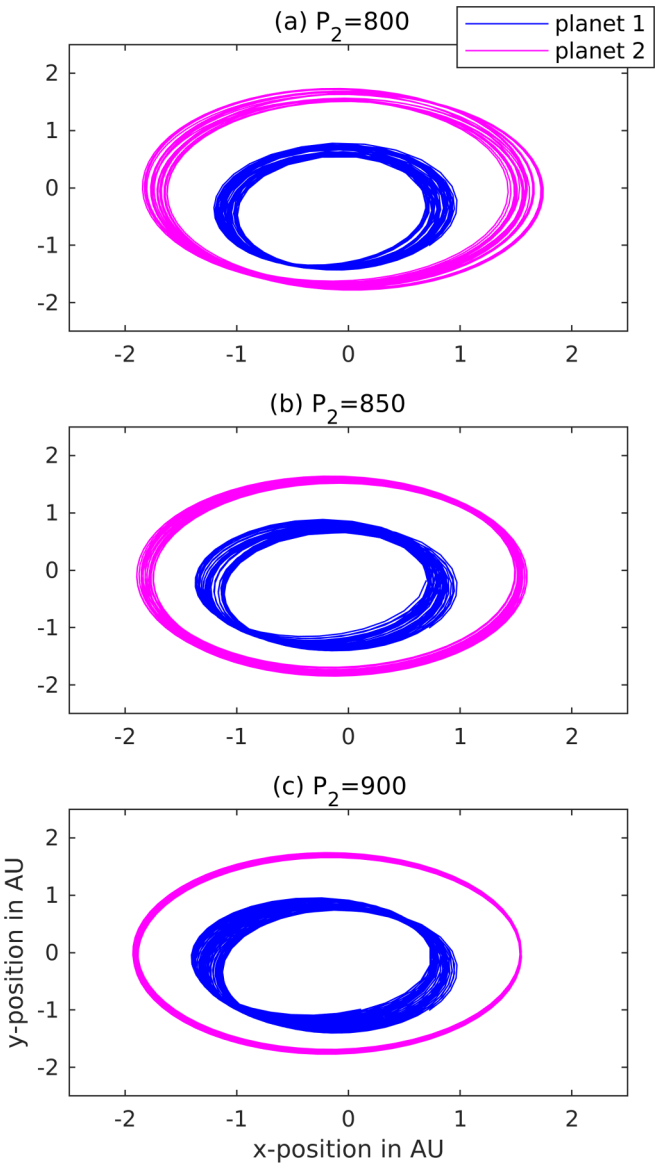

FIG. 10. Orbits traced out by the two planets over the simulation time of approximately 50 years, for three different values of the heavier planet's initial orbital period P_2. The initial eccentricity of the heavier planet is $e_2 = 0.1$, the other initial parameters are as in Ref. [30]. The position $(x = 0, y = 0)$ is the center of mass.

Here only a simple system of two planets in a coplanar setting was used as an example. However, the adapted correlation dimension method can also be employed on larger, nonplanar planetary systems, as we have shown in a recent study of the Trappist-1 system [33].

VI. CONCLUSION

Here we reported on a study that investigated an improved numerical method to determine the number of the classical integrals of motion. In particular, an adapted correlation dimension method [9] was used to determine the dimension ν of the

surface S upon which a trajectory evolves, and subsequently the number of integrals of motion. In contrast to previous studies, an additional step was added to the correlation dimension algorithm, which ensures that the method gives equal weight to different parts of the surface. As a consequence, the method yields the geometric dimension, needed to obtain the number of integrals of motion, yet it preserves the numerical efficiency of the correlation dimension methodology.

The resultant adapted correlation dimension method was used to determine the number of integrals of motion in the two degree of freedom Hénon-Heiles system, and to clearly distinguish between chaotic and regular dynamics. Results on a second test subject, an asymmetric top rigid molecule in an external electric field, showed that the algorithm works for rotational systems, and that it can follow an abrupt change of the number of integrals of motion as external parameters change. Furthermore, the existence of quasi-isolating integrals of motion in this system could be revealed.

In previous studies, the correlation dimension method yielded fractal numbers of integrals of motion for chaotic trajectories in the Hénon-Heiles system [3,5,6]. This had been interpreted as an indication that the trajectories move partially in a lower-dimensional regular regime and partially in a higher-dimensional chaotic regime. In this article, a different interpretation was demonstrated: The fractal dimension is a numerical artifact arising from trajectories hindered in their ergodic movement by partial barriers or turnstiles in the chaotic regions of phase space. In accord with this interpretation, for observation times much longer than the time needed to overcome these barriers one would expect a return to integer values for the dimension; this effect was indeed demonstrated. Furthermore, it was demonstrated that the adapted correlation dimension method may be used to determine the diffusion time for overcoming those partial barriers.

Finally, a new application of the correlation dimension method in predicting the long-time stability of planetary systems by using short-time observation was demonstrated. Remarkably, only 25 orbital cycles were needed for the prediction. Thus, with this method it may be possible to determine the long-time stability of astronomical systems using experimental data.

Here only low-dimensional examples were considered. There is no principal limitation to the dimensionality of systems that can be treated; however, as the number of points N needed for the correlation dimension algorithm increases with the dimension d, there are practical limitations. Although there is no general rule, it was suggested [13] that the number of points should approximately be $N = 10^{2+0.4d}$. Thus, for $N = 10^6$, which we found to be numerically still feasible, systems of dimensions up to $d = 10$ can be investigated; in a recent study we were able to characterize a seven-dimensional system [33]. Note that the embedding phase space can be of higher dimensionality.

We have also examined the possibility of directly extending this methodology to quantum mechanics. In doing so we have noted one significant impediment resulting from a specific feature of conservative classical mechanics. That is, every classical trajectory embodies the system's integrals of motion. As such, specifying an initial trajectory in phase space ensures that trajectory propagation will trace out the conserved manifold in phase space. The analogous situation does not appear to exist in quantum mechanics (e.g., for Bohmian trajectories [34]), necessitating a new approach to finding the number of integrals of motion of a quantum system. Such work is in progress.

ACKNOWLEDGMENTS

We thank Prof. I. Procaccia and Prof. H. Rein for helpful discussions. This work was supported by NSERC and by a fellowship within the Postdoc Program of the German Academic Exchange Service (DAAD). Computations were performed on the GPC supercomputer at the SciNet HPC Consortium. SciNet is funded by the Canada Foundation for Innovation under the auspices of Compute Canada, the Government of Ontario; Ontario Research Fund–Research Excellence, and the University of Toronto. Simulations in this paper made use of the REBOUND code, which can be downloaded freely at [35].

[1] G. Contopoulos, On the existence of a third integral of motion, Astron. J. **68**, 1 (1963).

[2] J. R. Stine and D. W. Noid, Method to determine the number of constants of the motion for multidimensional systems, J. Phys. Chem. **87**, 3038 (1983).

[3] P. Carnevali and P. Santangelo, Phase-space correlation functions and isolating integrals, Astrophys. J. **281**, 473 (1984).

[4] C. C. Martens and G. S. Ezra, A simple method for determining the number of isolating integrals in multidimensional systems: Computation of the pointwise dimension, Chem. Phys. Lett. **108**, 573 (1984).

[5] E. I. Barnes, Using correlation integrals to characterize three-dimensional stellar orbits, Astrophys. J. **559**, 736 (2001).

[6] D. D. Carpintero, Finding how many isolating integrals of motion an orbit obeys, Mon. Notices Royal Astron. Soc. **388**, 1293 (2008).

[7] M. Hénon and C. Heiles, The applicability of the third integral of motion: Some numerical experiments, Astron. J. **69**, 73 (1964).

[8] J. D. Farmer, E. Ott, and J. A. Yorke, The dimension of chaotic attractors, Physica D (Amsterdam) **7**, 153 (1983).

[9] P. Grassberger and I. Procaccia, Characterization of Strange Attractors, Phys. Rev. Lett. **50**, 346 (1983); Measuring the strangeness of strange attractors, Physica D (Amsterdam) **9**, 189 (1983).

[10] G. Contopoulos, A classification of the integrals of motion, Astrophys. J. **138**, 1297 (1963).

[11] J. Binney and S. Tremaine, *Galactic Dynamics*, 2nd ed. (Princeton University Press, Princeton, 2008).

[12] D. A. Russell, J. D. Hanson, and E. Ott, Dimension of Strange Attractors, Phys. Rev. Lett. **45**, 1175 (1980).

[13] J. C. Sprott, *Chaos and Time-Series Analysis* (Oxford University Press, Oxford, 2003).
[14] P. Grassberger, T. Schreiber, and C. Schaffrath, Nonlinear time sequence analysis, Inti. J. Bifurc. Chaos **01**, 521 (1991).
[15] D. L. Bunker, Monte Carlo calculation of triatomic dissociation rates. I. N_2O and O_3, J. Chem. Phys. **37**, 393 (1962).
[16] As a simple example consider a microscopic dust particle inside a bicycle tube: On short length scales it can freely move inside the tube and fill out a five-dimensional surface inside the six-dimensional phase space (the only isolating integral of motion being the conserved energy). However, looked upon using a length scale comparable to the diameter of the tube, the particle looks as if moving on a rigid ring, thus being limited to a two-dimensional surface in the phase space.
[17] T. L. Beck, D. M. Leitner, and R. S. Berry, Melting and phase space transitions in small clusters: Spectral characteristics, dimensions, and K entropy, J. Chem. Phys. **89**, 1681 (1988).
[18] P. Brumer and J. W. Duff, A variational equations approach to the onset of statistical intramolecular energy transfer, J. Chem. Phys. **65**, 3566 (1976).
[19] A. J. Lichtenberg and M. A. Liebermann, in *Regular and Chaotic Dynamics*, 2nd ed., edited by J. E. Marsden and L. Sirovich, Applied Mathematical Sciences Vol. 38 (Springer-Verlag, New York, 1992).
[20] R. S. Mackay, J. D. Meiss, and I. C. Percival, Transport in Hamiltonian systems, Physica D (Amsterdam) **13**, 55 (1984).
[21] J. D. Meiss, Symplectic maps, variational principles, and transport, Rev. Mod. Phys. **64**, 795 (1992).
[22] J. D. Meiss, Thirty years of turnstiles and transport, Chaos **25**, 097602 (2015).
[23] G. Contopoulos and M. Harsoula, Stickiness effects in conservative systems, Int. J. Bifurc. Chaos **20**, 2005 (2010).
[24] H. Goldstein, C. Poole, and J. Safko, *Classical Mechanics*, 3rd ed. (Addison Wesley, San Francisco, 2001).
[25] M. Arribas, A. Elipe, and M. Palacios, Quaternions and the rotation of a rigid body, Celestial Mech. Dyn. Astr. **96**, 239 (2006).
[26] J. Floß and P. Brumer, Laser-induced molecular alignment in the presence of chaotic rotational dynamics, J. Chem. Phys. **146**, 124313 (2017).
[27] M. Barrientos, A. Perez, and A. F. Ranada, Weak chaos in the asymmetric heavy top, Eur. J. Phys. **16**, 106 (1995).
[28] R. P. Butler, G. W. Marcy, S. S. Vogt, D. A. Fischer, G. W. Henry, G. Laughlin, and J. T. Wright, Seven new Keck planets orbiting G and K dwarfs, Astrophys. J. **582**, 455 (2003).
[29] S. S. Vogt, R. P. Butler, G. W. Marcy, D. A. Fischer, G. W. Henry, G. Laughlin, J. T. Wright, and J. A. Johnson, Five new multicomponent planetary systems, Astrophys. J. **632**, 638 (2005).
[30] H. Rein, Reanalysis of radial velocity data from the resonant planetary system HD128311, Mon. Notices Royal Astron. Soc. Lett. **448**, L58 (2015).
[31] H. Rein and S.-F. Liu, REBOUND: an open-source multi-purpose N-body code for collisional dynamics, Astron. Astrophys. **537**, A128 (2012).
[32] H. Rein and D. S. Spiegel, IAS15: a fast, adaptive, high-order integrator for gravitational dynamics, accurate to machine precision over a billion orbits, Mon. Notices Royal Astron. Soc. **446**, 1424 (2014).
[33] J. Floß, H. Rein, and P. Brumer, Dimensionality and integrals of motion of the Trappist-1 planetary system, Mon. Notices Royal Astron. Soc. **477**, 4874 (2018).
[34] P. R. Holland, *The Quantum Theory of Motion* (Cambridge University Press, Cambridge, 1993).
[35] http://github.com/hannorein/rebound.